

# Absolute distance measurements using FTPSI with a widely tunable IR laser

Leslie L. Deck  
Zygo Corporation  
Laurel Brook Road, Middlefield, CT. 06455-0448

## ABSTRACT

Fourier transform phase-shifting interferometry is further developed and applied to the absolute measurement of interferometer cavities. Using a widely tunable IR laser diode initially developed for telecom applications along with specific interferometer cavities, I apply this new capability to the measurement of absolute cavity lengths, where a  $1-\sigma$  precision of 12.6 ppb is demonstrated and the technique was then used to determinate the absolute index and thickness of a transparent parallel plate.

*Key words:* Interferometry, laser radar, metrology, FTPSI.

## 1 INTRODUCTION

Absolute distance interferometry via optical frequency modulation, often called chirped laser radar, has been typically demonstrated by tuning the injection current of laser diodes<sup>1,2</sup>, however these attempts have been plagued with problems associated with the stability of the lasing medium, a relatively short tuning range (typically less than 20GHz) and intensity nonuniformity stemming from injection tuning. Lasers manufactured for telecom sparing applications solve most of the problems that limited the range and accuracy of previous attempts. Tunable telecom lasers are extraordinary devices, packaged in rugged, self-contained modules with Telcordia mandated lifetime specifications and recently exhibiting mode-hop free tuning ranges in excess of 40nm (5THz) with linewidths of a few hundred kHz. They run single mode and mode-hop free, exhibit little intensity variation during the tune, have generally more power than visible diodes, come conveniently fiber pigtailed which produces a high quality wavefront and are easy to tune. An additional benefit is their longer wavelength, producing a longer fringe order ambiguity range.

In a previous publication, I described a new phase-shifting technique called Fourier transform phase-shifting interferometry<sup>3</sup> (FTPSI<sup>4</sup>) for high precision measurements of surfaces in the presence of multiple-surface interference<sup>5</sup>. FTPSI uses wavelength-tuning in conjunction with specific cavity geometries to minimize the spectral overlap of higher order multiple interference, thereby reducing phase errors associated with spectral contamination. The technique is capable of high precision measurements of surface profiles, optical and physical thickness variation and homogeneity variation including, for the first time, homogeneity wedge<sup>6</sup>. In this paper, I extend the capabilities of FTPSI to the absolute measurement of interferometer cavity lengths with the help of a widely tunable laser initially designed for telecom applications. After establishing the accuracy of the technique by measuring the length of a well known cavity to nanometer precision, the method is used to determine the absolute index and thickness of a parallel plate.

## 2 ABSOLUTE DISTANCE USING WAVELENGTH SHIFTING INTERFEROMETRY

A single elemental (2-surface) cavity observed in a reflective Fizeau geometry is depicted in Figure 1. Light rays enter the cavity from the left and reflect off the two parallel surfaces separated by a physical gap  $G_C$  containing a medium with refractive index  $n_C$ . The total phase difference between light rays reflected from the first surface and light rays which traverse the optical gap  $2M$  times is given by

$$\Phi = 2Mn_C G_C \frac{2\pi\nu}{c} + \Theta, \quad (1)$$

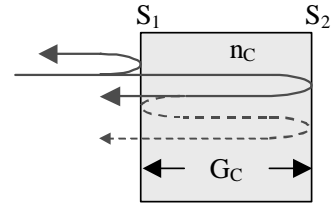


Figure 1: An elemental 2-surface cavity

where  $\nu$  is the optical frequency of the light and  $M$  is called the interference order and is equal to 1 for 1<sup>st</sup> order interference. For convenience, phase changes upon reflection at the surfaces have been lumped into the constant  $\Theta$ . Tuning the source optical frequency produces a 1<sup>st</sup> order interference frequency  $f_C$  of,

$$f_C = \frac{L_C \dot{\nu}}{c} [1 + \eta_c], \quad (2)$$

where  $\dot{\nu}$  is the optical frequency tuning rate,  $L_C = 2n_C G_C$  is the total OPL of the 1<sup>st</sup> order cavity and the term  $\eta = \frac{\nu}{n} \frac{\partial n}{\partial \nu}$  is due to the index chromatic dispersion. The  $\eta$  term cannot be ignored even though the actual wavelength shift may be small<sup>7</sup>. For fused silica at 1550nm,  $\eta$  is approximately 1.3%. Eq. (2) is the fundamental equation governing the interferometric frequency evolution in an elemental cavity containing a dispersive medium.

## 3 ABSOLUTE FOURIER TRANSFORM PSI

As surfaces are added to the interferometer cavity, the observed interferogram is a linear superposition of the interferograms from the combinatorial collection of all possible elemental cavities. A cavity consisting of  $N$  surfaces contains  $N-1$  primary gaps (the physical gap between adjacent surfaces),  $N(N-1)/2$  1<sup>st</sup> order interference frequencies and many more higher-order frequencies. In the form described in Ref. 4, FTPSI provides the ability to measure surface profiles in the presence of multiple surface interference by analyzing the interferograms acquired during wavelength tuning in the Fourier domain. As long as the frequencies are well separated, a complete Fourier analysis of the interferogram can extract the 1<sup>st</sup> order frequencies and calculate the spatial phase variations for all the elemental cavities with a single wavelength-tuned acquisition. It was shown that this frequency separation could be guaranteed if the test cavity were constructed appropriately.

In this application, we wish to measure the absolute thickness and index of a transparent flat. A cavity geometry shown in Figure 2 is chosen where the plate thickness is the largest elemental cavity in order to minimize the length, and hence atmospheric turbulence, in the remaining air gaps. To eliminate the influence of spurious frequencies below the expected noise floor of the apparatus, the cavity is constructed to separate multiple surface reflections up to 3<sup>rd</sup> order from the 1<sup>st</sup> order frequencies. These requirements imply making  $G_2$  the largest cavity and setting the other two gaps to



Figure 2: The 4-surface cavity geometry

$$\begin{aligned}
G_3 &= G_2 / (M + 1) \\
G_1 &= G_3 / (M + 1) = G_2 / (M + 1)^2 .
\end{aligned}
\tag{3}$$

Figure 3 shows the frequency spectrum predicted for this cavity geometry and a 500GHz tune. The 2<sup>nd</sup> and 3<sup>rd</sup> order spectra are included to highlight the excellent frequency separation achieved. Of the six 1<sup>st</sup> order peaks, only the first three, corresponding to gaps  $G_1$ ,  $G_3$  and  $G_2$  respectively, will be needed in the following analysis.

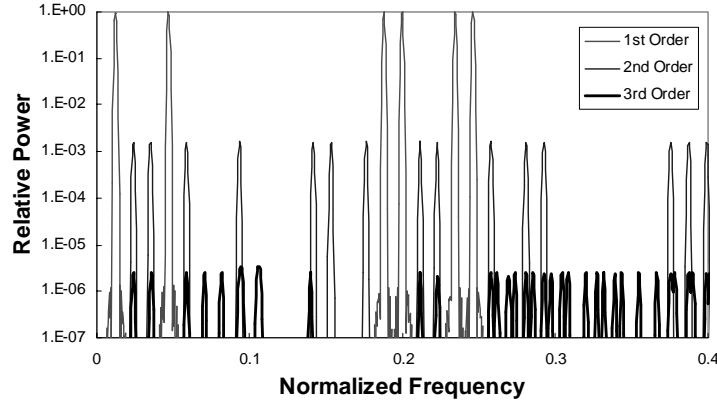


Figure 3: Log plot of the 1<sup>st</sup> (red), 2<sup>nd</sup> (blue) and 3<sup>rd</sup> (black) order spectra for a 4-surface cavity geometry with  $M=3$  and a 500GHz tune. The frequency is normalized to the sample rate. Note the higher order frequencies are well separated from the 1<sup>st</sup> order peaks.

In FTPSI, the 1<sup>st</sup> order frequencies of each of the elemental cavities are identified in the measured spectrum and the spatial phase distribution  $\varphi$  is recovered from the complex amplitude of the Fourier transform of the interference time history  $a(t)$  evaluated at the corresponding cavity frequency.

$$\varphi = \arg(A(f_c)),
\tag{4}$$

with

$$A(f_c) = \int_{-\infty}^{\infty} a(t)w(t)\exp(-i2\pi f_c t)dt ,
\tag{5}$$

where  $f_c$  is a particular 1<sup>st</sup> order elemental cavity interference frequency and  $w(t)$  is the Fourier window function chosen to bandwidth-limit the signal. The spectrum is calculated via

$$S(f) = |A(f)|^2 .
\tag{6}$$

The measurement of an optical gap entails determining the frequency  $f$  for which Eq. (6) is a maximum. However, this formulation assumes that the tuning is perfectly linear, allowing the definition of a constant interference frequency. As the optical frequency tune departs from linearity, the spectrum will shift and distort, producing errors in

the frequency determination. Nonlinear tuning effects are a practical reality, so a separate high precision wavelength monitor is incorporated to account for this<sup>8</sup>. The monitor consists of a separate interferometer cavity of known, fixed OPL  $L_M$  and the interference intensity of this cavity is obtained simultaneously with the main interferometer cavity during the tune. Additionally, a special Fourier transform, called the OPL transform, is defined that accounts for nonlinear tuning and dispersion and extracts the optical distance directly.

From Eq. (2), the 1<sup>st</sup> order interference frequency observed by the wavelength monitor is,

$$f_M = \frac{L_M \dot{\nu}}{c} [1 + \eta_M]. \quad (7)$$

Since both the interferometer and the monitor cavities experience the same tuning rate, Eqs. (2) and (7) give,

$$f_C = \frac{L_C [1 + \eta_C]}{L_M [1 + \eta_M]} f_M. \quad (8)$$

Thus, the monitor provides a high precision, independent measure of the wavelength change and can account for both nonlinear tuning effects as well as optical power variations occurring during the tune. Combining Eqs. (5) and (8), affecting the change of variables  $t \rightarrow \varphi_M$  using  $\varphi_M = 2\pi f_M t$ , and converting to discrete time signals, we can write,

$$A(L_C) = \sum_{j=0}^{N-1} a_j w_j \exp\left(-i\varphi_{Mj} \frac{L_C [1 + \eta_C]}{L_M [1 + \eta_M]}\right) \Delta\varphi_{Mj}. \quad (9)$$

where the index  $j$  runs over the  $N$  intensity samples  $a_0 \dots a_N$ . Eq. (9) is called the OPL transform. As with the Fourier transform, an OPL spectrum  $S$  can be generated via,

$$S(L) = |A(L)|^2. \quad (10)$$

with each peak in the spectrum corresponding to the OPL of a particular elemental cavity. Furthermore, analogously to Eq (6), the phase variation for a cavity with an OPL of  $L_C$  can be calculated with

$$\varphi_C = \arg[A(L_C)]. \quad (11)$$

The optical gap of an elemental cavity is then found by the OPL position at the extremum of the appropriate OPL spectrum peak. The OPL transform requires accurate knowledge of the phase evolution of the wavelength monitor cavity, which is provided by analyzing the monitor interference history with a Sliding Discrete Fourier Transform (Sliding DFT).<sup>9</sup>

In a manner similar to the Fourier analysis of interference produced by broad-band sources<sup>10</sup>, the OPL determined by the spectral peak position can be refined by using the phase calculated from Eq. (11). In effect, the fringe order is determined using the “coarse” calculation of the OPL derived from the spectrum peak and is combined with the high resolution phase measurement to refine the OPL determination to fractions of a fringe. The phase determined by Eq. (11) is modulo  $2\pi$ , thus we can write

$$\varphi_C + 2\pi N = kL_C + \pi, \quad (12)$$

where  $N$  is the fringe order,  $k$  is the wavenumber ( $k = 2\pi/\lambda$ ) and the last  $\pi$  is due to the phase change on reflection from one of the dielectric surfaces bounding the cavity (the last surface for air gaps or the 1<sup>st</sup> surface for the test flat cavity). Using Eq. (12), the fringe order is determined using the coarse measurement of  $L_C$  with

$$N = \text{round} \left[ \frac{kL_C + \pi - \varphi_C}{2\pi} \right]. \quad (13)$$

where the round function finds the nearest integer to its argument. A refined measurement of the OPL,  $\bar{L}_C$ , using the high precision measurement of the phase can then be made with,

$$\bar{L}_C = \frac{2\pi N - \pi + \varphi_C}{k}. \quad (14)$$

This procedure requires that the uncertainty in the coarse OPL measurement be significantly less than  $\lambda$ .

Armed with high accuracy measurements of the gap OPLs, the absolute thickness of the test flat  $G_2$  can be found with

$$G_2 = \frac{L_{EC} - L_3 - L_1}{2n_{air}}, \quad (15)$$

where  $L_{EC}$  is the OPL of the empty cavity (a measurement taken with the flat removed) and  $n_{air}$  is the index of the air during the measurement. The test flat refractive index can be simply calculated via,

$$n = \frac{L_2}{2G_2}. \quad (16)$$

The measurement procedure can be summarized in the following seven steps;

- 1) Acquire test cavity and monitor interference data while tuning the source wavelength.
- 2) Calculate the monitor phase evolution using the Sliding DFT.
- 3) Determine the OPL spectrum with Eq. (10) and identify the spectral peak associated with the gap.
- 4) Calculate a coarse OPL for each gap from the spectrum maxima and determine the fringe order using this coarse OPL measurement.
- 5) Refine the OPL using the phase determined from Eq. (11).
- 6) Repeat steps 1-4 for the empty cavity (test flat removed).
- 7) Calculate the absolute thickness and index using Eqs. (15) and (16).

The precision possible with this technique is quite extraordinary. Assuming a precision of a few nanometers in the absolute cavity measurements, as is demonstrated below, measurements of the index to a few ppb are possible. Furthermore, a spatial map of the absolute index is easily obtained either by direct measurement across the part or by combining the results of an absolute measurement at one point with the index variation profile obtained from Standard FTPSI.

## 4 EXPERIMENTAL VERIFICATION

Absolute measurements with FTPSI were experimentally demonstrated using the apparatus shown in Figure 4. The apparatus consisted of a conventional phase-shifting Fizeau interferometer equipped with a tunable telecom laser and wavelength monitor. The returning interferogram was split; a part directed to a 320x240 InGaAs camera (the Merlin from Indigo Systems) to obtain standard 2-dimensional interferograms for FTPSI analysis, the other part

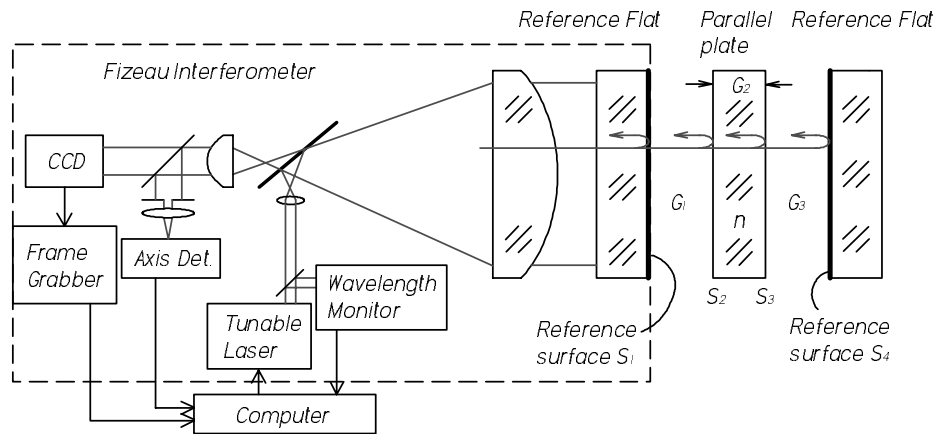


Figure 4: Apparatus used in the experiments to perform the measurements.

apertured to cover only a small area about the optical axis and directed to a single point detector. The test cavity consisted of a test flat mounted between two reference flats with the gaps between surfaces set to those mandated by the optimum cavity geometry prescribed previously. The tunable source was a Lambda Light DFB laser with integrated thermo-electric cooler (TEC) from QDI (Yorba Linda, CA.), thermally tunable from 1554 to 1558nm (500GHz). The

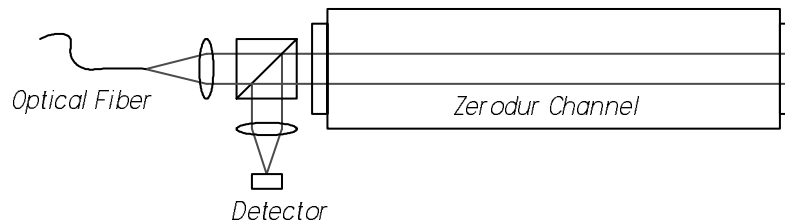


Figure 5: The wavelength monitor

tuning was accomplished by applying a voltage waveform to the adjustable temperature set point of a HyTek HY5650 TEC controller powering the laser TEC. The voltage waveform was preset to a profile that minimized the open-loop tuning nonlinearity.

The wavelength monitor (WM), shown in Figure 5, consisted of a fixed length Fabry-Perot cavity. The cavity was constructed out of 30mm square Zerodur rectangular bar with a 10mm diameter center hole. The ends of the bar were polished flat and parallel and two wedged windows optically contacted to the bar ends. The bar length was measured with a tactile probe (LaserRuler, by Pratt & Whitney) to be  $237.1704 \pm 0.0005$  mm with an expected thermal dependence of  $25\text{nm}/^\circ\text{C}$ . Figure 6 shows a typical

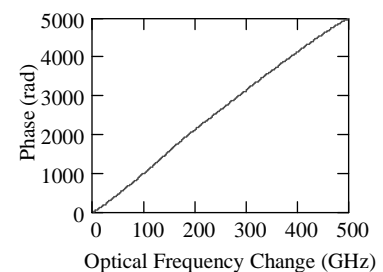


Figure 6: The monitor phase variation in a typical 500GHz tune.

wavelength monitor phase variation from a Sliding DFT analysis during a typical tune, the remaining nonlinearity was less than 4% of full scale. This phase data is applied to the OPL transform, thereby automatically compensated for the remaining tuning nonlinearities in the FTPSI analysis.

#### 4.1 Absolute distance measurements

The absolute gap of a single elemental cavity was first attempted to validate the technique. A second Fizeau cavity similar to the wavelength monitor was constructed out of Zerodur. The ends were polished flat and parallel and the gap was measured with the tactile probe to be  $237.2147 \pm 0.0005$ mm. Two wedged flats were optically contacted to the ends of the Zerodur channel to complete the cavity. The cavity was measured 80 times over the course of 8 hours. Figure 7 shows the OPL spectrum (Eq. (12)) from a typical measurement. The ratio of the instrument noise floor to the peak is about  $10^{-7}$ . This is about an order of magnitude lower than the expected amplitude of 3<sup>rd</sup> order frequencies (Figure 3), validating the need to provide a geometry that separates multiple interference out to 3<sup>rd</sup> order.

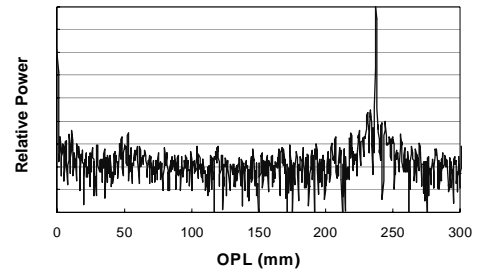


Figure 7: Measured OPL spectrum from the elemental cavity after a 500GHz tune.

Figure 8 shows the results of the 80 Zerodur cavity measurements. The length of the cavity was measured to be  $237.214301 \pm 0.000003$  mm (1- $\sigma$ ), in agreement with the tactile probe measurement (the dashed line) and constituting

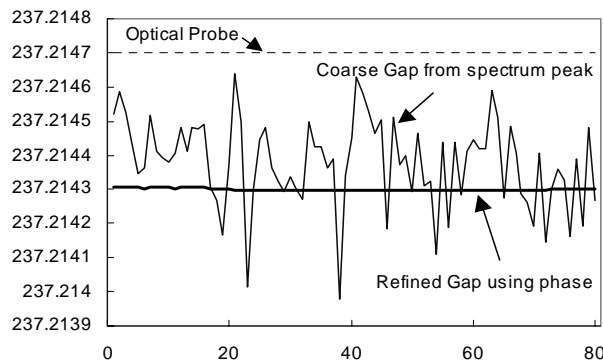


Figure 8: Length measurement of the Zerodur cavity.

a physical length measurement precision of 12.6 ppb. The uncertainty of the measurement depends mainly on the uncertainty in the length of the wavelength monitor cavity, which is 2.1ppm (500nm).

#### 4.2 Absolute thickness and index of a flat

A parallel flat made of Fused silica  $84.2809 \pm 0.0005$ mm thick was used to test the technique for the determination of thickness and index. With an expected index of 1.444 at 1550nm wavelengths, the optical thickness of the flat was therefore 123mm. The optical gaps  $G_1$  and  $G_3$  as determined from Eq. (14), were set close to 7.5mm and 30mm respectively. Figure 9 is a log plot of the OPL spectrum from the intensity variation seen by the on-axis detector during a 500GHz tune. When comparing this spectrum with the

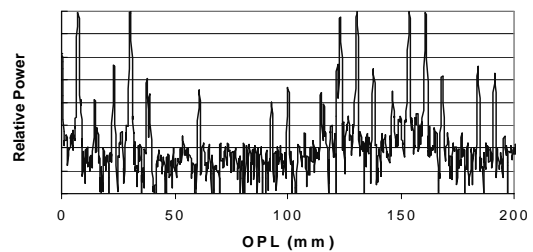


Figure 9: Log of measured OPL spectrum from the test cavity after a 500GHz tune.

theoretical spectrum in Figure 3, it is easy to identify the OPLs of the 1<sup>st</sup> and 2<sup>nd</sup> order interference cavities, while the 3<sup>rd</sup> order amplitudes are mainly hidden near the noise floor. The coarse position of each of the 1<sup>st</sup> order peaks, as determined by finding the point where the slope was zero, is in excellent agreement with the theoretically expected positions, indicating that the cavity was correctly constructed to minimize multiple interference effects to 3<sup>rd</sup> order. Figure 10 shows the OPL spectrum of the empty cavity measurement.

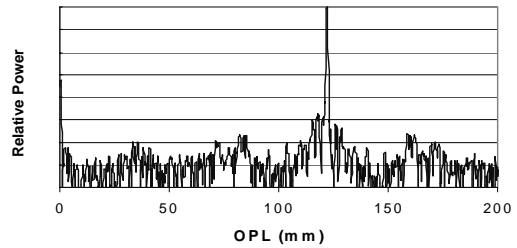


Figure 10: Log of measured OPL spectrum from the empty cavity after a 500GHz tune.

The requirement of a time-separated empty cavity measurement is a weakness of the technique since changes in the physical alignment of the two reference surfaces in the interval between the two measurements will lead to measurement errors. The sensitivity of the physical thickness measurement to these errors is one-to-one. In order to minimize the time between full and empty cavity measurements, the full cavity was always performed first, eliminating alignment adjustments between acquisitions. Figure 11 shows

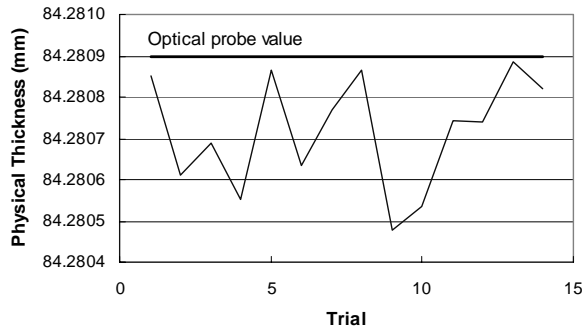


Figure 11: Measured physical thickness of the 84mm transparent flat compared to the optical probe value.

the results of 14 measurements of the thickness of the test flat over a two-day interval. The air temperature and pressure were recorded during this time to correct the monitor OPL for atmospheric index changes. Using the known coefficient of thermal expansion for fused silica of  $5.5e-7/^{\circ}C$ , the flat thickness was expected to change by less than 15nm during this time. The average value of 84.28072mm agrees well with the tactile probe measurement, but the scatter (140nm rms) is significantly worse than that one might hope for from the optical gap results. The variation is completely due to cavity changes occurring between the full and empty cavity measurements. This problem can be

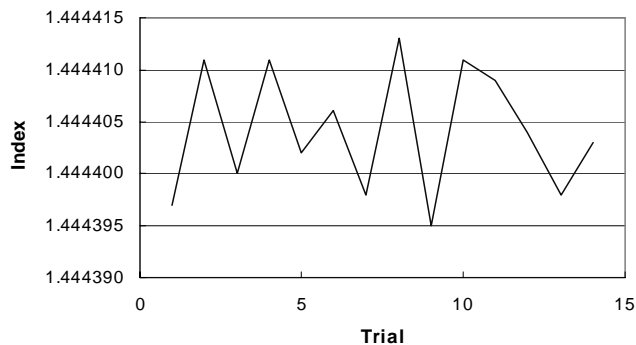


Figure 12: Measured index of the 84mm transparent flat, 1.444404.

theoretically eliminated if the flat is smaller than the observable aperture because the area surrounding the plate can then serve as an indicator of cavity changes between the two measurements. Any changes in the relative orientation of last two surfaces can be measured and compensated for during the analysis. This procedure was attempted but the problem currently encountered with this approach is that the electronic filtering characteristics of the camera produced frequency dependent phase distortions in the OPL spectrum that reduced the precision of the fringe order calculation. Future work in this area is planned.

The index evaluated with Eq. (16) for this series of 14 measurements is shown in Figure 12. The average value is  $1.444404 \pm 0.000006$ . The value is in agreement with the calculated value using the dispersion formula determined by Malitson<sup>11</sup>, but the actual value at 1550nm for this sample was unknown. Most of the scatter stems from the variation in the absolute thickness. With a temperature sensitivity of  $1.28e-5/^{\circ}\text{C}$ , the actual variation in the index is expected to be less than 0.000002 over the measurement series.

## 5 SUMMARY

I show in this paper how Fourier transform phase-shifting interferometry in conjunction with a widely tunable telecom laser diode can be adapted to the task of high-precision measurements of absolute optical distances. The technique was demonstrated with the measurement of the physical length of a 237mm cavity to 3nm  $1\sigma$ , a measurement precision of 12ppb. With this capability established I show how to use the method for the high precision measurement of the absolute thickness and index of a parallel plate.

## REFERENCES

- <sup>1</sup> H. Kikuta, K. Iwata, R. Nagata, "Distance measurement by the wavelength shift of laser diode light," *Appl. Opt.*, **25**, 2976-2980 (1986)
- <sup>2</sup> A. J. den Boef, "Interferometric laser rangefinder using a frequency modulated diode laser," *Appl. Opt.*, **26**, 4545-4550 (1987)
- <sup>3</sup> L. Deck, "Measurements using Fourier-Transform Phase Shifting Interferometry," *Proc. ASPE* **25**, 115-118 (2001)
- <sup>4</sup> FTPSI is the topic of US and Foreign patents pending assigned to Zygo Corporation
- <sup>5</sup> L. Deck, "Simultaneous Multiple Surface Measurements using Fourier-Transform Phase Shifting Interferometry," in: 4<sup>th</sup> International workshop on automatic processing of fringe patterns, Fringe 2001, Elsevier, Paris, (2001), 230-236
- <sup>6</sup> L. Deck, "Multiple Surface Phase Shifting Interferometry," *Proc. SPIE*, **4451**, 424-430 (2001)
- <sup>7</sup> P. de Groot, "Chromatic dispersion effects in coherent absolute ranging," *Opt. Lett.* **17**, 898-900 (1992)
- <sup>8</sup> S. Egorov, I. Likhachev, A. Mamasev, A. Polyantsev, "Fiber-optic sensors with a nonlinear frequency modulation of the optical carrier," *Tech. Phys. Lett.*, **19**, 169-170 (1993)
- <sup>9</sup> J. Tsui, "Digital techniques for wideband receivers," 1<sup>st</sup> Edition, Chap. 4.8.2, Boston, MA: Artech House (1995)
- <sup>10</sup> P. de Groot and L. Deck, "Surface profiling by analysis of white-light interferograms in the spatial frequency domain," *J. Mod. Opt.*, **42**, 389-401 (1995)
- <sup>11</sup> I. H. Malitson, "Interspecimen comparison of the refractive index of Fused Silica," *JOSA*, **55**, 1205-1209 (1965)